Chemical Engineering and Processing 97 (2015) 187–194

Contents lists available at ScienceDirect

Chemical Engineering and Processing: Process Intensification

journal homepage: www.elsevier.com/locate/cep

Understanding temperature-induced primary nucleation in dual impinging jet mixers

Mo Jiang, Chen Gu, Richard D. Braatz*

Massachusetts Institute of Technology, 77 Massachusetts Avenue, Cambridge, MA 02139, USA

ARTICLE INFO

Article history:
Received 7 May 2015
Accepted 16 June 2015
Available online 6 July 2015

Keywords:
Micromixers
Nucleation
Dual impinging jets
Process intensification
Boundary layer theory
Crystallization

ABSTRACT

The discovery that crystal nuclei can be generated by combining hot and cold saturated solutions in a dual-impinging-jet (DIJ) mixer motivates the theoretical analysis in this article. Nucleation is shown to be facilitated in solute–solvent systems that have much higher energy transfer than mass transfer rates near the impingement plane between the two jets. One- and two-dimensional spatial distributions of velocity, temperature, concentration, and supersaturation provide an improved understanding of primary nucleation in cooling DIJ mixers. In the most important spatial region for characterization of nucleation, the two-dimensional fields are shown to be very close to analytical solutions derived from a one-dimensional approximation of the energy and molar balances. This simplification enables the derivation of design criteria that facilitates assessment of whether any particular solute–solvent combination will nucleate crystals in a cooling DIJ mixer, based on the physicochemical properties of the system. These criteria could save time and material by avoiding or reducing trial-and-error experiments, which is helpful at the early stage of pharmaceutical process development.

1. Introduction

A key objective in pharmaceutical crystallization is to control the crystal size distribution (CSD), to improve process efficiency and product quality. An effective way to improve the control of CSD is through combining continuous seeding and growth with concentration control [1]. One well-studied approach for continuous seeding is to combine solution and anti-solvent streams in a dual-impinging jet (DIJ) mixer [1–5]. The underlying principle is that, at appropriate flow rates, such a DIJ mixer can generate high-intensity micro-mixing of fluids to quickly achieve a nearly spatially homogeneous composition of high supersaturation before the onset of primary nucleation. An inexpensive DIJ mixer can be used to rapidly generate a large production rate of small crystals and remove any need for post-crystallization milling, which simplifies the overall manufacturing process and avoids a potential route for the generation of an undesirable polymorphic transformation [2,3].

Rather than anti-solvent crystallization as commonly used, a cooling DIJ mixer was recently demonstrated that combined hot and cold saturated solutions under laminar flow conditions to generate small uniform seed crystals of an organic compound [6]. All of the crystals from the cooling DIJ mixer were about 10 μm in length, placing them in the approximate size range for direct application in inhalers [7]. Theoretically, if the mixing was perfect (that is, solution concentrations and temperature were completely mixed at the molecular scale in the mixer), the average supersaturation level in Ref. [6] was too low to nucleate the crystals in a cooling DIJ mixer. The surprising result of nucleating crystals by combining hot and cold saturated solutions in a DIJ mixer motivates the theoretical analysis of the system in this article. Also, it would be useful at the early stage of process research and development to be able to quickly decide on compound–solvent combinations for DIJ mixers without the time-consuming trial-and-error experiments that are currently used [4]. These two motivations lead to the main objectives of this article: (i) to improve the understanding of primary nucleation under laminar flow conditions in cooling DIJ mixers, and (ii) to develop design criteria for cooling DIJ mixers to quickly rule out unsuitable compound–solvent combinations based on their physicochemical properties. The primary emphasis is on the free-surface DIJ mixer configuration, which is simple and flexible to implement experimentally [8], although the results are relevant to other DIJ mixer configurations operating under laminar flow conditions.

A mathematical model is developed for a DIJ mixer that combines thermodynamics, kinetics, fluid dynamics, and heat and mass transfer. The mathematical model is in the form of partial differential equations, simplified by exploiting symmetries and employing scaling analysis. The theoretical analysis is supported

* Corresponding author. Fax: +1 617 253 3112.
E-mail address: braatz@mit.edu (R.D. Braatz).

http://dx.doi.org/10.1016/j.cep.2015.06.013
0255-2701/

with process simulation. The two-dimensional energy and molar balances are solved using COMSOL given an analytical solution for the velocity field, to generate spatial distributions of temperature, concentration, and supersaturation near the hot–cold interface within a cooling DIJ mixer. Compared to past work with similar DIJ geometries (e.g., confined dual jets) that mainly used numerical simulations to investigate flow and heat/mass transfer characteristics [1,9–12], analytical expressions are derived that provide physical insight, which are compared and supported with numerical results. Based on these analytical solutions of velocity, temperature, and concentration spatial distributions, design criteria are developed for assessing the feasibility of crystal nucleation in cooling DIJ mixers for specific pharmaceutical–solvent combinations, and for choosing operating conditions to increase the probability of primary nucleation.

2. Theory

An analytical solution for the local flow field near the interface between two impinging jets can be derived for a partial differential equation simplified by exploiting symmetries. Assumptions are presented and justified that are subsequently used to determine temperature and concentration spatial distributions via analytical and numerical approaches.

2.1. Assumptions with justifications for deriving an analytical solution of the DIJ local velocity field

A schematic of a DIJ mixer is shown in Fig. 1a, with an example set of operating parameters in Table 1 and the analytically computed jet shape for laminar flow conditions in Fig. S1. Nucleation can only occur very close to the impingement plane between the two jets, since the supersaturation is zero far from the impingement plane and can only be significantly greater than zero when the jets are close enough to transfer heat and solute with each other. The region with the highest potential of nucleation is of most interest, which is where the residence time is the longest, shown as an orange box in Fig. 1a and referred to as 'local' here. Like some past studies that have mathematically modeled similar geometries (e.g., single free-surface jet impingement on a normal plane [13–15] or dual-impinging jets [16]), three assumptions are made to simplify the analysis:

(i) The fluid is assumed to be laminar, irrotational, and in steady state.
(ii) The flow is assumed to be axisymmetric and the two impinging jets are assumed to have the same velocity field but in opposing directions.
(iii) The flow is assumed to be incompressible with constant values of density and viscosity.

In the experimental study that demonstrated the nucleation of crystals by mixing hot and cold saturated solutions [6], the Reynolds number indicates that the flow was in a laminar regime, which is the regime of interest in this article. As an example, the Reynolds number at the exit, $Re = \rho UL/\mu$, is on the order of 600 (using jet velocity v_z and inner diameter $2r_0$, with density and dynamic viscosity values in Table 2) or smaller [17]. No splattering is expected at such a low Reynolds number [18].

The axisymmetric assumption simplifies the analysis while being a good approximation for free liquid (unconfined) opposed-jet DIJ configuration with a flow rate ratio of 1:1. The two jet flows are considered symmetric with respect to the impingement plane (aka contact plane between the low temperature/low concentration fluid and the high temperature/high concentration fluid), with each side of the impingement plane being a jet of circular cross-section of radius R (Fig. 1a and b). The symmetry allows the convenient use of cylindrical coordinates (Fig. 1a), where the z direction is that of jet centerline (positive direction on the right side of the impingement plane), and the r direction is perpendicular to z, pointed outward from the centerline. The angular velocity parallel to the interface (v_θ) is zero.

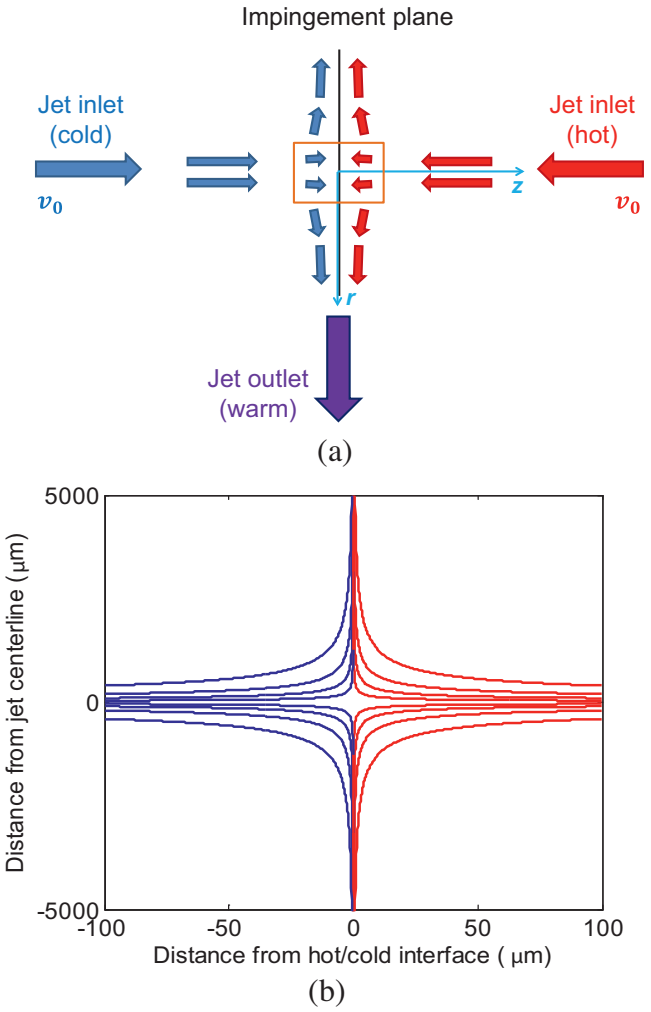

Fig. 1. (a) Schematic of a free-surface cooling DIJ mixer. The centerlines of hot (70 °C, red, right side) and cold (25 °C, blue, left side) jets align. Both jets have the same volumetric flow rate, so the impingement plane is a symmetry plane perpendicular to the jet centerline. (b) Streamlines of the hot (red, right side) and cold jets (blue, left side) of the cooling DIJ mixer in (a), from the analytical solutions of the flow field (1) and (2). (For interpretation of the references to color in this figure legend, the reader is referred to the web version of this article.)

The assumption of spatially uniform density simplifies the analysis while being a good approximation for the impingement of two saturated solutions containing the same solute and solvent. As a specific example, the density of LAM aqueous solution (or slurry with very small amount of nuclei) in Table 1 is a weak function of temperature and concentration, so the densities for cold, hot, and mixed LAM solutions/slurries are nearly identical, and of similar magnitude as the density of water at the average temperature. Liquid flow with uniform density is incompressible by definition. The dynamic viscosity of LAM aqueous solution is a stronger function of solute concentration and temperature compared to density, but in this DIJ configuration, the viscosity difference between hot and cold streams does not affect the velocity field (which is proved in the solution key to question 9–10b in Ref. [16]).

Table 1
Experimental parameters for the cooling crystallization of L-asparagine monohydrate (LAM, from Sigma–Aldrich) in a free-surface DIJ mixer with aligned centerline [8].

Physical properties	Values
Molecular weight (g/mol)	150.13
Hot jet temperature, T_{hot} (°C)	70
Hot jet concentration, c_{hot} (g LAM/g water)	0.20 (slightly supersaturated)
Cold jet temperature, T_{cold} (°C)	25
Cold jet concentration, c_{cold} (g LAM/g water)	0.03 (saturated)
Area-average jet velocity, v_z (m/s)	1.9 (or slightly higher)
Inner diameter of the jet nozzle, $2r_0$ (μm)	254
Jet nozzle-to-interface distance, z_0 (μm)	5000
The largest distance away from the centerline at interface, R (μm)	5000

The relation between the solubility of LAM in deionized (DI) water (c_{sat}, in g LAM/g water) and temperature (T, in °C) is $c_{sat} = 3.084 \times 10^{-2} T - 1.373 \times 10^{-3} T + 5.214 \times 10^{-5} T^2$ [6]. Thus the solubility of LAM at the average mixing temperature (approximately 47.5 °C, the average of the temperatures of two streams) is about 0.08 g LAM/g water.

Table 2
Physical constants associated with the crystallization of glycine in water [23].

Physical properties	Values
Density, ρ (kg/m^3)	977.8 (70 °C), 997.1 (25 °C)
Dynamic viscosity, μ (N s/m^2)	0.4×10^{-3} (70 °C), 0.58×10^{-3} (47.5 °C), 0.9×10^{-3} (25 °C)
Thermal conductivity, k (mW/m K)	663.1 (70 °C), 607.2 (25 °C)
Heat capacity, C_p (kJ/kg K)	4.19 (70 °C), 4.18 (25 °C)
Thermal diffusivity, $\alpha = k/\rho C_p$ (m^2/s)	1.6×10^{-7} (70 °C), 1.5×10^{-7} (25 °C)
Diffusion coefficient of glycine in water at infinite dilution, D (cm^2/s)	1.05×10^{-5} (25 °C)
Acceleration due to gravity, g (m/s^2)	9.81

The temperature and concentration variations are small and do not affect the velocity field.

2.2. Analytical solution of the DIJ local velocity field

Under the assumptions, the velocity field derived using streamline analysis is [16]

$$v_r = -\frac{1}{r}\frac{\partial \psi}{\partial z} = Cr \ (>0) \tag{1}$$

$$v_z = \frac{1}{r}\frac{\partial \psi}{\partial r} = -2Cz \ (<0 \text{ for } z>0) \tag{2}$$

As an example of the determination of the constant C, consider an experimental system with a nozzle-to impingement plane distance of $z = z_0 = 5$ mm with a jet velocity along the jet centerline of $v_{z_0} = -1.9$ m/s; then the constant C determined from Eq. (2) is $C = -v_{z_0}/2z_0 = 190\ s^{-1}$. A momentum boundary layer does not develop, as there are no sharp gradients in the velocity field where two jets impinge.

2.3. Assumptions for calculation of temperature and concentration spatial fields

The temperature and concentration spatial distribution of liquid within a DIJ mixer is calculated via both analytical and numerical approaches. The governing equations of heat and mass transfer up to the incidence of nucleation is

$$v_r\frac{\partial T}{\partial r} + v_z\frac{\partial T}{\partial z} = \alpha\left[\frac{1}{r}\frac{\partial}{\partial r}\left(r\frac{\partial T}{\partial r}\right) + \frac{\partial^2 T}{\partial z^2}\right] \tag{3}$$

$$v_r\frac{\partial c}{\partial r} + v_z\frac{\partial c}{\partial z} = D\left[\frac{1}{r}\frac{\partial}{\partial r}\left(r\frac{\partial c}{\partial r}\right) + \frac{\partial^2 c}{\partial z^2}\right] \tag{4}$$

where α is thermal diffusivity and D is the molecular diffusivity. The boundary conditions for the temperature $T(r, z)$ are

$$\frac{\partial T}{\partial r}(0,z) = 0,\ T(r,z_0) = T_{hot} = 70\ °C,\ T(r,-z_0) = T_{cold} = 25\ °C \tag{5}$$

where some example temperature values are given. For the experimental configurations of interest, the boundary conditions can be approximated to very high accuracy by

$$\frac{\partial T}{\partial r}(0,z) = 0,\ T(r,\infty) = T_{hot} = 70\ °C,\ T(r,-\infty) = T_{cold} = 25\ °C.$$

The corresponding boundary conditions for concentration $c(r, z)$ are

$$\frac{\partial c}{\partial r}(0,z) = 0,\ c(r,\infty) = c_{hot} = 0.20\ \text{g LAM/g water},\ c(r,-\infty) = c_{cold} = 0.03\ \text{g LAM/g water}, \tag{6}$$

where some example concentration values are given.

For both the heat and mass transfer Eqs. (3) and (4), assume that (i) the analytical solution for the velocity field (1) and (2) is valid for the region of interest (Fig. 1a); (ii) the air/liquid interfaces are assumed to be streamlines from the analytical solution for the velocity field, starting from the edge of the inlet nozzles; (iii) the thermal diffusivity α is approximated as a constant. Assumption (iii) is a very accurate approximation for most systems; for example, α varies by less than ±3.5% and the molecular diffusivity D is constant over a wide range of temperature for the system in Table 2.

All numerical simulations were made using the finite element method as implemented in COMSOL V4.3, using two additional assumptions:

(i) Uniform temperature and concentration at the nozzle inlets.
(ii) No mass or heat flux at the air/liquid interfaces (including very far from centerline).

The latter assumption holds because air is an excellent insulator. One-dimensional analytical solutions involve additional

approximations described in the next section, where the analytical solutions are derived and compared to the numerical simulations.

3. Results and discussion

This section employs scaling analysis to simplify the heat and mass transfer equations from two dimensional (2D) to one dimensional (1D) so that relatively simple analytical solutions can be derived. The approach employs boundary layer theory, as concentration and thermal boundary layers arise due to the large difference in concentration and temperature in the two impinging jets, which generates large spatial gradients near the impingement plane. For the region of interest, the 1D analytical solutions are shown to be comparable to the 2D numerical solutions except near the outlet flows. Based on the analytical solutions for the temperature and concentration spatial fields, the supersaturation profile is analyzed for regions of high potential for nucleation, which leads to design criteria for inducing nucleation in cooling DIJ mixers.

3.1. Flow field and residence time

A good understanding of the velocity field is a prerequisite for the analysis of heat and mass transfer. The fluid flows are decelerated in the radial direction while approaching the impingement plane (Eqs. (1) and (2), Fig. 1a), and diverted radially and accelerated in the radial direction, due to the fluid mass balance and finite volume of the region of interest (orange box in Fig. 1a, with small r and z). Eqs. (1) and (2) are analytical expressions for the velocity field that are valid for the region of interest.

The liquid velocity in the z-direction is very small near the impingement plane, making the residence time very large for liquid moving along the jet centerline (Fig. 1b). According to Eqs. (1) and (2), the residence time exactly on the jet centerline is infinite. In reality, liquid will not flow exactly along the centerline (due to molecules having finite size, small fluctuations, etc.), so the residence time of a fluid element in the zone of interest is finite but still much longer than any other fluid regions.

3.2. Scaling analysis for the temperature and concentration spatial distributions

The independence of the heat and mass transfer governing Eqs. (3) and (4) enables independent analysis. In the region of interest

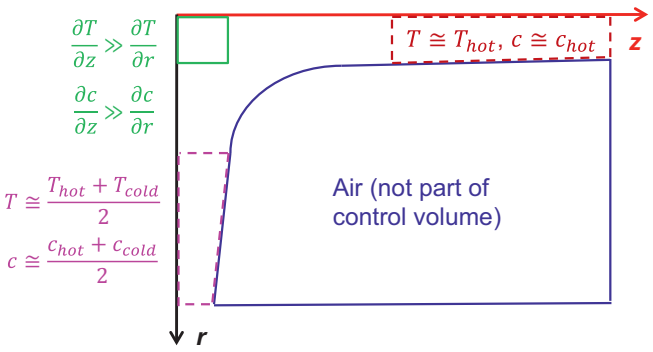

Fig. 2. Schematic for scaling analysis and defining the region of interest (only the hot jet side is shown due to symmetry). The z axis is the jet centerline. The blue region (large r,large z) is air, which is not in the control volume. Temperatures and concentrations in the purple (large r, small z) and brown (large z, small r) regions are approximately spatially uniform, serving as boundary conditions (with values listed). The green region (small r, small z) of low velocity and long residence time is of interest for nucleation. (For interpretation of the references to color in this figure legend, the reader is referred to the web version of this article.)

(Fig. 2), the temperature gradient along impingement plane ($\partial T/\partial r$) is negligible compared to along the centerline ($\partial T/\partial z$) because the dominating direction of heat transfer (conduction) is from hot jet to cold jet [16]. In this way, the two-dimensional energy conservation Eq. (3) can be simplified to a one-dimensional equation,

$$v_z \frac{\partial T}{\partial z} = \alpha \frac{\partial^2 T}{\partial z^2}, \tag{7}$$

along the centerline. This simplified equation has the unique analytical solution [16]

$$\frac{T - T_{cold}}{T_{hot} - T_{cold}} = \frac{1}{2}\left(\mathrm{erf}\left(\frac{z}{z_{refh}}\right) + 1\right) \tag{8}$$

where $z_{refh} = \sqrt{\alpha/C}$. For the system in Table 2, $z_{refh} = 28.1$ μm.

This analytical solution (8) is in the form of an error function, indicating a sharp temperature gradient at the impingement plane ($z = 0$) and high nonlinearity along the axial direction (Fig. 3c). The error function also indicates temperature gradient drops to nearly zero at a distance of about z_{refh} from the impingement plane (supported by Fig. 3a–c). For the region of interest (near $r = z = 0$), the 1D analytical solution (Fig. 3c) generates a very similar temperature profile to the 2D simulation from COMSOL (Fig. 3b), which confirms the validity of the scaling analysis used to derive the 1D analytical solution.

Similar scaling analysis applies for the concentration field, to give

$$v_z \frac{\partial c}{\partial z} = D \frac{\partial^2 c}{\partial z^2} \tag{9}$$

Similar to the temperature equation, the simplified concentration Eq. (9) has the unique analytical solution [16]

$$\frac{c - c_{cold}}{c_{hot} - c_{cold}} = \frac{1}{2}\left(\mathrm{erf}\left(\frac{z}{z_{refm}}\right) + 1\right) \tag{10}$$

where $z_{refm} = \sqrt{D/C}$. For the system in Table 2, $z_{refm} = 2.35$ μm.

The assumptions and governing equations for heat and mass transfer are very similar, and heat transfer is decoupled from mass transfer, thus the analytical solutions for the temperature and concentration profiles (8) and (10) are expected to be very similar. The trend of the concentration variation is very similar to the temperature, with sharp gradient at the impingement plane and nonlinear gradient along the z axis as shown in Figs. 3 and 4. For the region of interest, the 1D analytical model (Fig. 4c) generates a very similar concentration profile to the 2D simulation from COMSOL (Fig. 4b). Thus for assessing the potential of primary nucleation, the analytical model is sufficiently accurate.

The difference between heat and mass transfer exists in the length scale along centerline (in the example system, $z_{refh} = 28.1$ μm for the temperature gradient change, and $z_{refm} = 2.35$ μm for the concentration gradient change, as shown in Figs. 3–5), which comes from the difference in heat and mass transfer rates. This difference can be indicated by the large value of Lewis number ($Le = 143$), which is the ratio between thermal diffusivity and mass diffusivity (α/D), and also the ratio of the Schmidt number to the Prandtl number.

3.3. Supersaturation spatial distribution and design criteria

The supersaturation spatial distribution was calculated (Figs. 5 and 6) based on the analytical solutions for the temperature and concentration profiles in the region of interest (Figs. 3c and 4c). Due to the different heat and mass transfer rates, the temperature of the hot solution can drop toward the average temperature of the

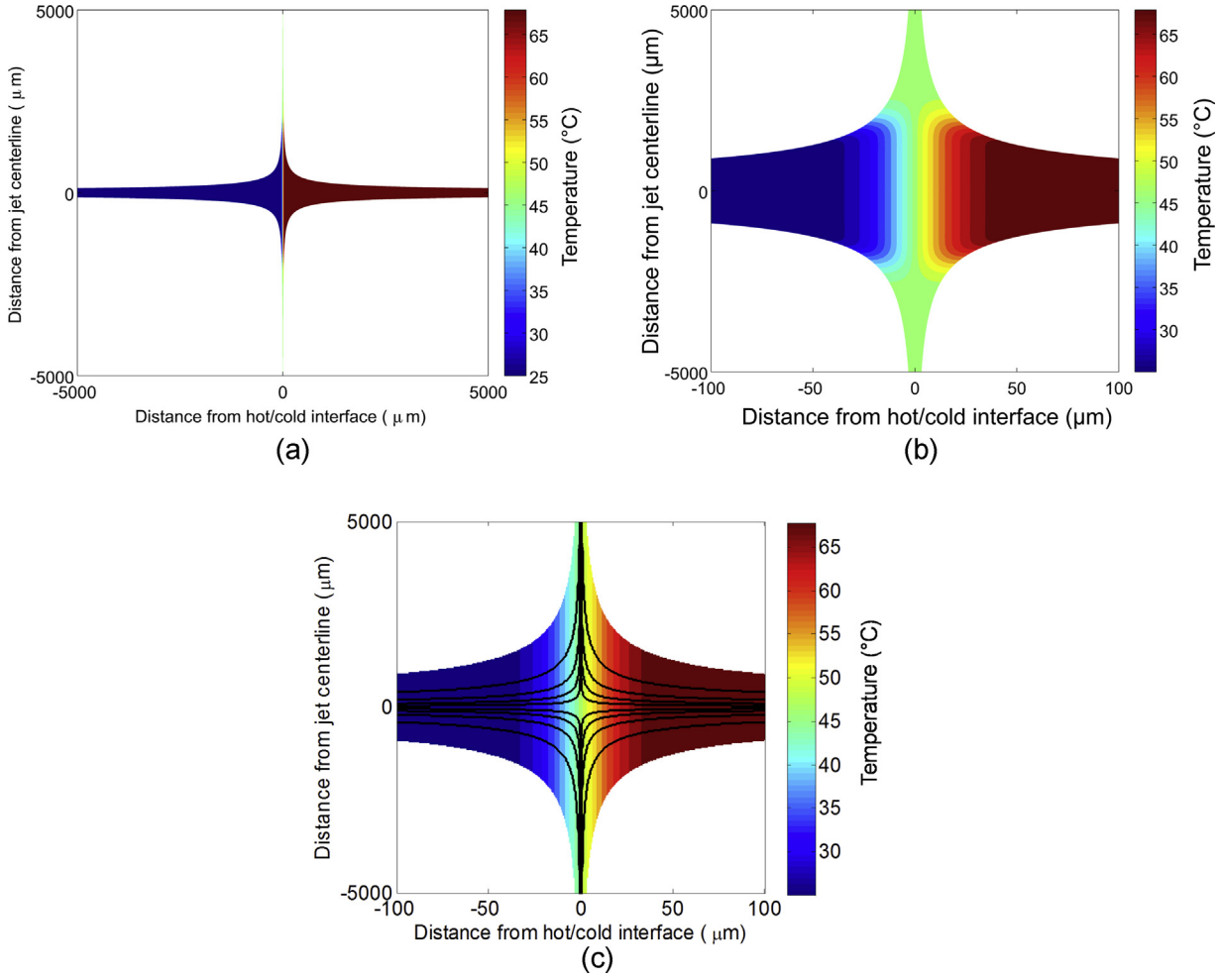

Fig. 3. Temperature field: (a) computed by 2D simulation using the finite element method implemented in COMSOL, at the full length range with the dimensions being the nozzle-to-nozzle distance and the contact area diameter; (b) computed by 2D simulation using the finite element method implemented in COMSOL, very near the impingement plane (small range of z, as if 'stretching' (a) horizontally); (c) 1D analytical solution near the impingement plane, with the streamlines shown in black. The temperature is indicated by color (red indicates high temperature, and blue indicates low temperature), in unit of °C, and the black lines are streamlines. The cold impinging jet is on the left, and the hot impinging jet on the right. The white color shows air at room temperature. The edges between air and liquid are streamlines starting from the edge of the inlet nozzles. (For interpretation of the references to color in this figure legend, the reader is referred to the web version of this article.)

two solutions before its solution concentration has significantly changed (Fig. 5). Supersaturation can be much higher than the spatially averaged supersaturation (e.g., 0.035 g LAM/g water) near the impingement plane at the hot stream side (e.g., 0.10 g LAM/g water, from Fig. 6 or Region A in Fig. 7), where the temperature (and the solubility) is low while the concentration remains high (Figs. 5 and 7). Between the impingement plane and Region A on the hot stream side (marked as Region B in Fig. 7), the residence time is very high (due to low velocity) with positive supersaturation (though not as high as in Region A).

The high local supersaturation with long local residence time encourages the nucleation of crystals in a DIJ mixer by combining hot and cold saturated solutions. This analysis leads to two design considerations for preferentially nucleating in a cooling DIJ mixer:

(i) Calculate the Lewis number for the solute/solvent system. A large value of α/D favors the generation of a region of high supersaturation (Region A in Fig. 7).
(ii) Choose inlet temperatures and concentrations for the two jets so that the average supersaturation is as high as possible at the set jet velocity (or flow rate) ratio. For 1:1 ratio of flow rates from the two jets, the average concentration of hot and cold streams should be set as high as possible relative to the solubility at the average temperature, that is, so that the inequality $1/2(C_{hot} + C_{cold}) > C_{sat,T_{hot}+T_{cold}/2}$ holds with as large of a gap as possible.[1]

Region A can be related to a metastable limit obtained from a batch crystallization experiment. The average of the inlet jet concentrations does not need to be above the metastable limit in the crystallization phase diagram for nucleation to occur, but the peak concentration in the spatial domain should be. The metastable zone width in a benchtop well-mixed tank experiment will be lower than the metastable zone width in a dual-impinging jet experiment, due to the larger volume and the presence of a stirring blade in the well-mixed tank [19]. To induce nucleation in a dual-impinging jet mixer, the maximum concentration should be higher than the metastable limit at its corresponding temperature, which is described by the analytical expression

[1] The inequality is almost always satisfied for organic compounds with convex solubility curves, such as LAM for the concentrations in Table 1, 1/2 (0.2 + 0.03) = 0.115 > 0.08.

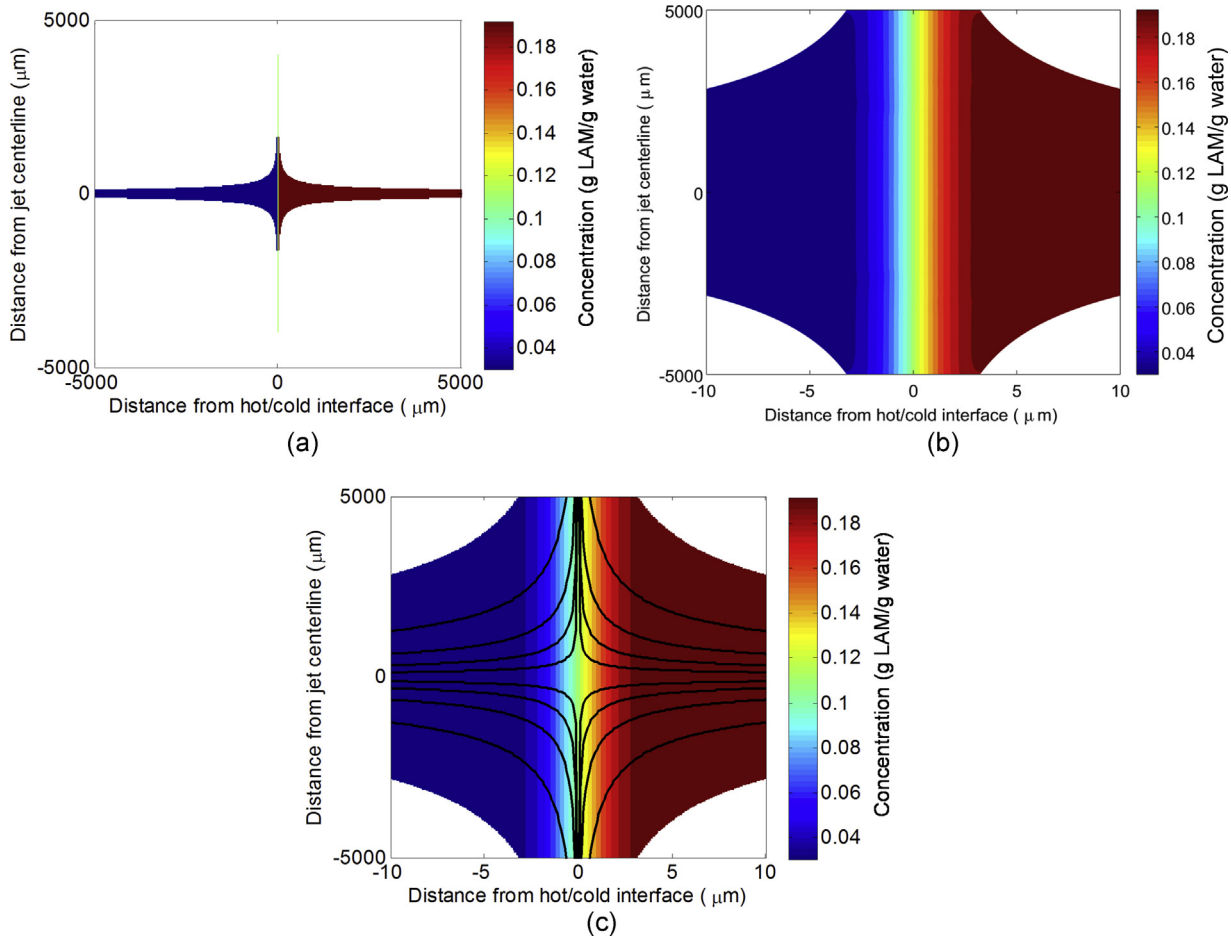

Fig. 4. Concentration field: (a) computed by 2D simulation using the finite element method implemented in COMSOL, at the full length range (same as in Fig. 3a); (b) computed by 2D simulation using the finite element method implemented in COMSOL, very near the impingement plane; (c) 1D analytical solution near the impingement plane, with the streamlines shown in black. The concentration is indicated by color (red indicates high concentration, and blue indicates low concentration), in unit of g LAM/g water. As in Fig. 3, the cold impinging jet is on the left and the hot impinging jet on the right, and the edges between air and liquid are streamlines starting from the edge of the inlet nozzles. The streamlines in (c) (black) are the same as in Fig. 3c. (For interpretation of the references to color in this figure legend, the reader is referred to the web version of this article.)

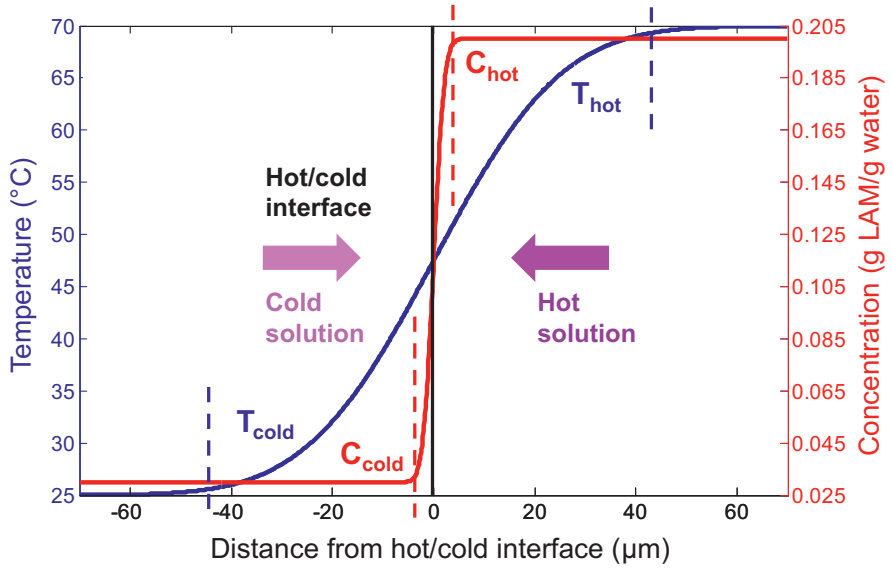

Fig. 5. Temperature (blue) and concentration (red) profiles (solid lines) and edges of the boundary layers (dashed lines), based on the 1D approximation (Figs. 3c and 4c) along the jet centerline. The black line is the impingement plane. (For interpretation of the references to color in this figure legend, the reader is referred to the web version of this article.)

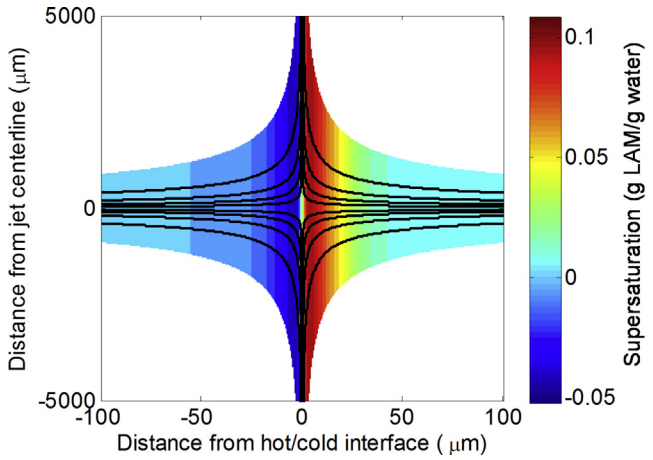

Fig. 6. Supersaturation spatial field for the cooling DIJ mixer based on the 1D analytical solutions (Figs. 3c and 4c). The streamlines in black are the same as in Figs. 3c and 4c. The absolute supersaturation is indicated by color (red indicates high supersaturation, and blue indicates low supersaturation), in unit of g LAM/g water. (For interpretation of the references to color in this figure legend, the reader is referred to the web version of this article.)

$$\max_z\left\{\frac{1}{2}\left(\mathrm{erf}\left(\frac{z}{z_{refm}}\right)+1\right)-\frac{c_{\mathrm{meta}}(T(z))-c_{\mathrm{cold}}}{c_{\mathrm{hot}}-c_{\mathrm{cold}}}\right\}>0, \tag{11}$$

which is derived from the 1D analytical solution (10) for the concentration.

For a particular system, if this condition (11) does not hold, then it is very unlikely that nucleation will occur in the cooling DIJ mixer. Several approaches are available to increase the potential for primary nucleation. One approach to increase both the peak supersaturation and the left-hand side term in Eq. (11) is to increase c_{hot} by making the hot solution supersaturated (but not so supersaturated as to nucleate when standing in its feed tank). If aggregation or oiling out phenomena is observed during DIJ mixing, then the concentration at the high temperature should be reduced.

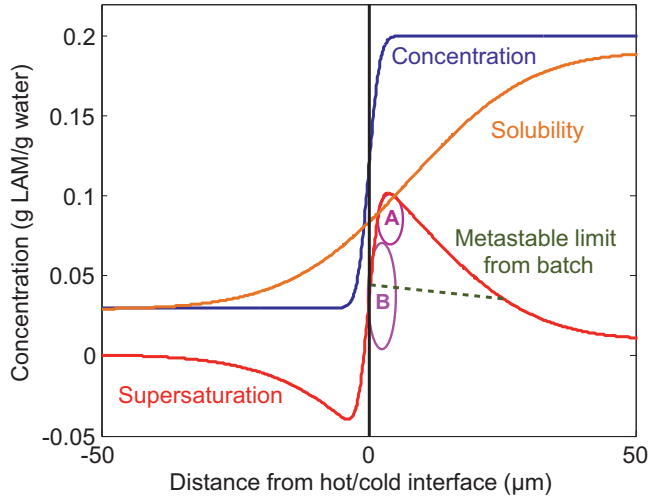

Fig. 7. Concentration (blue curve), solubility (dark orange curve) and supersaturation (red curve) profiles along the jet centerline based on the 1D analytical solutions. Region A (dark purple) is the high supersaturation region, located between the thermal and concentration boundary layers, closer to the latter. Region A is just above the metastable limit for cooling DIJ, which is higher than the metastable limit in a cooling bath (dark green dashed line) due to smaller volume and faster cooling rate. Region B (light purple) is a long residence time region with slow velocity, located very near the jet centerline and the impingement plane. (For interpretation of the references to color in this figure legend, the reader is referred to the web version of this article.)

A second approach to facilitate primary nucleation is to reduce the inlet jet velocity (but not so low that the jets no longer impinge). Lowering the jet velocity increases the residence time (the C in Eq. (1) becomes smaller and the z_{refm} in Eq. (11) becomes larger).

Another approach is to increase the nozzle-to-impingement plane distance z_0 to decrease C and increase z_{refm}. The use of this approach is limited as longer distance will make the jet centerline alignment more difficult. When using the second and third approaches, the dependency of c_{meta} on z should be taken into account.

4. Conclusions

The primary nucleation of crystals by combining saturated hot and cold solutions in a cooling DIJ mixer is analyzed, mostly in terms of derived analytical expressions for the velocity, temperature, concentration, and supersaturation fields. The analytical solutions with a 1D approximation of the temperature and concentration fields are accurate in the region of interest, as confirmed by 2D numerical solutions by the finite element method.

Design criteria were developed to provide guidance for achieving nucleation within a cooling DIJ mixer: (i) the Lewis number $\alpha/D \gg 1$, so that the heat transfer is much faster than mass transfer, and (ii) the solute concentration on the hot side of the interface should be higher than the metastable limit. The higher heat transfer rate than mass transfer rate enables the temperature of the hot solution to drop to approximately the average temperature of the two solutions before its solution concentration had significantly dropped, resulting in a supersaturation sufficiently high to nucleate crystals even at low spatially averaged supersaturation. Several approaches were suggested to facilitate nucleation: (i) increase the concentration of the hot inlet stream, (ii) decrease the inlet jet velocity; and (iii) increase the distance between the two jets. The design criteria provide guidance, at the early stage of process development, for researchers to quickly identify compound–solvent combinations that will not nucleate crystals within DIJ mixers, based on their physicochemical properties.

The analysis of the cooling DIJ mixer may be extended to other free-surface DIJ mixer configurations such as the use of oblique angles between the inlet nozzles or flow rate ratios other than 1:1. In the latter case, the symmetry analysis and flow field calculations will be different [13,15,20,21]. The design criteria involve principles that are more general than the specific assumptions used in their derivation, and may also provide guidance to other devices that generate small uniform-sized crystals through mixing hot and cold streams, such as radial or coaxial mixers [22].

Acknowledgements

The authors thank Prof. William M. Deen, Prof. Jeremy VanAntwerp, Guolong Su, Jianjian Wang, Zeyuan Zhu, Jun Fu, and Lucas Charles Foguth for helpful technical input and discussion. Novartis is acknowledged for financial support.

Appendix A. Supplementary data

Supplementary data associated with this article can be found, in the online version, at http://dx.doi.org/10.1016/j.cep.2015.06.013.

References

[1] X.Y. Woo, R.B.H. Tan, R.D. Braatz, Precise tailoring of the crystal size distribution by controlled growth and continuous seeding from impinging jet crystallizers, CrystEngComm 13 (6) (2011) 2006–2014.
[2] M. Midler Jr., E.L. Paul, E.F. Whittington, M. Futran, P.D. Liu, J. Hsu, S.H. Pan, Crystallization method to improve crystal structure and size. U.S. Patent #5314506 A, May 24, 1994.

[3] B.K. Johnson, R.K. Prud'homme, Chemical processing and micromixing in confined impinging jets, AIChE J. 49 (9) (2003) 2264–2282.
[4] H.-H. Tung, E.L. Paul, M. Midler, J.A. McCauley, Crystallization of Pharmaceuticals: An Industrial Perspective, Wiley, Hoboken, NJ, 2009.
[5] R. Dauer, J.E. Mokrauer, W.J. Mckeel, Dual jet crystallizer apparatus. U.S. Patent #5578279, November 26, 1996.
[6] M. Jiang, M.H. Wong, Z. Zhu, J. Zhang, L. Zhou, K. Wang, A.N. Ford Versypt, T. Si, L.M. Hasenberg, Y.E. Li, R.D. Braatz, Towards achieving a flattop crystal size distribution by continuous seeding and controlled growth, Chem. Eng. Sci. 77 (2012) 2–9.
[7] N. Rasenack, H. Steckel, B.W. Muller, B.W. Müller, Micronization of anti-inflammatory drugs for pulmonary delivery by a controlled crystallization process, J. Pharm. Sci. 92 (1) (2003) 35–44.
[8] M. Jiang, Pharmaceutical Crystallization Design Using Micromixers, Multiphase Flow, and Controlled Dynamic Operations. Ph.D. Thesis, Massachusetts Institute of Technology, Cambridge, Massachusetts, 2015.
[9] Y. Wu, Impinging Streams: Fundamentals, Properties, Applications, Elsevier/Chemical Industry Press, Amsterdam/Beijing, China, 2007.
[10] Y. Liu, R.O. Fox, CFD predictions for chemical processing in a confined impinging-jets reactor, AIChE J. 52 (2) (2006) 731–744.
[11] E. Gavi, D.L. Marchisio, A.A. Barresi, CFD modelling and scale-up of confined impinging jet reactors, Chem. Eng. Sci. 62 (8) (2007) 2228–2241.
[12] S.M. Hosseinalipour, A.S. Mujumdar, Flow and thermal characteristics of steady two dimensional confined laminar opposing jets: part I. Equal jets, Int. Commun. Heat Mass Transf. 24 (1) (1997) 27–38.
[13] B.W. Webb, C.F. Ma, Single-phase liquid jet impingement heat transfer, Adv. Heat Transf. 26 (1995) 105–217.
[14] D.J. Phares, G.T. Smedley, R.C. Flagan, The inviscid impingement of a jet with arbitrary velocity profile, Phys. Fluids 12 (8) (2000) 2046–2055.
[15] C.duP. Donaldson, R.S. Snedeker, Study of free jet impingement. Part 1. Mean properties of free and impinging jets, J. Fluid Mech. 45 (1971) 281–319.
[16] W.M. Deen, Analysis of Transport Phenomena, 2nd ed., Oxford University Press, New York, 2012.
[17] J.M. Bergthorson, K. Sone, T.W. Mattner, P.E. Dimotakis, D.G. Goodwin, D.I. Meiron, Impinging laminar jets at moderate Reynolds numbers and separation distances, Phys. Rev. E 72 (6) (2005) 66307.
[18] J.H. Lienhard V, Heat transfer by impingement of circular free surface liquid jets. Proceedings of the 18th National and 7th ISHMT-ASME Heat and Mass Transfer Conference, IIT, Guwahati, India, January 2006. Available online: http://web.mit.edu/lienhard/www/jets.pdf.
[19] L. Goh, K. Chen, V. Bhamidi, G. He, N.C.S. Kee, P.J.A. Kenis, C.F. Zukoski, R.D. Braatz, A stochastic model for nucleation kinetics determination in droplet-based microfluidic systems, Cryst. Growth Des. 10 (6) (2010) 2515–2521.
[20] S. Devahastin, A.S. Mujumdar, A numerical study of flow and mixing characteristics of laminar confined impinging streams, Chem. Eng. J. 85 (2–3) (2002) 215–223.
[21] D.A. Johnson, Experimental and numerical examination of confined laminar opposed jets part I. Momentum imbalance, Int. Commun. Heat Mass Transf. 27 (4) (2000) 443–454.
[22] M. Jiang, Z. Zhu, E. Jimenez, C.D. Papageorgiou, J. Waetzig, A. Hardy, M. Langston, R.D. Braatz, Continuous-flow tubular crystallization in slugs spontaneously induced by hydrodynamics, Cryst. Growth Des. 14 (2) (2014) 851–860.
[23] W.M. Haynes (Ed.), CRC Handbook of Chemistry and Physics, 93rd ed., CRC Press/Taylor and Francis, Boca Raton, FL, 2013 Available online: http://www.hbcpnetbase.com (accessed 22.05.13).